

Adsorption behaviours of phenols onto high specific area activated carbon derived from *Trapa bispinosa*

Kaman Singh^{1*} & Bhuwan Chandra²

¹Surface Science Laboratory, Faculty of Science, Department of Chemistry, University of Lucknow 226 007, India

Advanced Center of Surface Chemistry, Department of Applied Chemistry,

²School for Physical Sciences, Babasaheb Bhimrao Ambedkar University (A Central University), Lucknow 226 025, India

E-mail: drkamansingh@yahoo.com

Received 3 January 2014; accepted 19 June 2014

A low cost activated carbon derived from an aquatic plant *Trapa bispinosa* (TB) residue, has been characterized for the removal of phenol and its derivatives (*p*-chlorophenol and *p*-nitrophenol) from their aqueous solutions. The derived *Trapa bispinosa* husk (TBH) has micro porous and meso porous pore size distribution with high surface area ($454 \text{ m}^2 \text{ g}^{-1}$) and high carbon content (77%). The Langmuir, Freundlich, Redlich-Peterson and Temkin models have been applied to evaluate the adsorption parameters. The possible adsorption interactions have been discussed. The effects of pH, urea and ionic strength on the adsorption suggest that the adsorption of phenols is attributed to hydrogen bonding; however, hydrophobic interactions and charge transfer interactions are also believed to be responsible for the observed adsorption in the present case. The adsorption decreases in the order of *p*-chlorophenol > phenol > *p*-nitrophenol. Thermodynamic study demonstrates an endothermic nature of adsorption. Adsorption kinetics is examined using different kinetics model (Lagergren first order and pseudo second order). The best results have been achieved with the Langmuir isotherm equilibrium model and followed pseudo second order kinetics ($R^2 = 0.99$). The TBH is found to be very effective for removal of phenols from their aqueous solutions.

Keywords: Low cost activated carbon, Lagergren first order, Pseudo second order, *Trapa Bispinosa*

Phenol and its derivatives are hazardous materials for living beings¹, which are released into the aquatic environment by industries such as oil, gasoline, coal, paper, textile, petrochemicals, pharmaceuticals, phenolic resin, plastics, leather, tanning, wood, paint and fertilizer. Phenols causes taste and odour problems to drinking water² which invites many problems to human health including diarrhea, liver damage, anemia and dark urine³. There are various methods available for the treatment processes for phenols from wastewater such as chemical (oxidation, solvent extraction, irradiation, coagulation)^{4,5} biological (accumulation, microbial degradation)⁶ and physical methods (adsorption, bioadsorption, activated carbon)⁷⁻¹¹. However, in recent years, adsorption systems have been widely employed in the purification of wastewater. The content of phenolic compounds in industrial wastewater (~200-2000 mg /L) is usually higher than the standard limits (mostly 0.5 mg/L) established for their release into the aquatic environment¹². Consequently, extensive research work has been carried out using activated carbons and resins¹³. Many researchers^{9,14} have shown that activated carbon is an effective adsorbent for

organic compounds, especially for phenol and its derivatives. However, its application for the treatment of wastewaters is not economical. Taking these criteria into consideration, the search for a low cost and easily available adsorbents has led many investigators to seek more economic and efficient techniques using natural and vegetal adsorbents¹⁵⁻²⁰.

The objective of the present work was to evaluate the analytical potential of TBH for effective removal of phenol and its derivatives from their aqueous solutions. The physical and chemical properties of the TBH were evaluated and the effect of solution pH, temperature, urea and ionic strength of adsorption was studied.

Experimental Section

All reagents used were AR-grade chemicals. Stock solutions of the test solutions were made by dissolving phenol, *p*-chlorophenol, and *p*-nitrophenol in double distilled water. The pH of the test solutions was adjusted using dilute HCl (0.1 N) and NaOH (0.1 N). The TBH was derived from an inexpensive, abundantly available and eco-friendly vegetal source.

Preparation of activated carbon (TBH) from the *Trapa bispinosa*

The fruit of *Trapa bispinosa* (TB) obtained from the local area of Lucknow, Uttar Pradesh (India) was used as a precursor for activated carbon employing HNO₃ activation method. The raw material was washed with tap water to remove any ashes on the surface, dried and crushed in a pestle and mortars. The dried mass was immersed in 35 wt% HNO₃ at a ratio of 3:1 over 12 h at 60°C, followed by carbonization and activation at 510°C in a muffle furnace for 1 h. After cooling, the produced material was washed several times with distilled water until a constant near neutral pH was observed, then dried at 85°C for 8 h, cooled to room temperature, and sieved to the desired particle size by standard sieves. The product was referred to as TBH.

Equipment

The TBH (2 mg) was mixed with 200 mg of KBr and then pelleted. The FT-IR spectra of the pellets were recorded using a Fourier Transform Infra-Red Spectrometer (FTIR) of ThermoScientific (Nicole 6700). The particle morphologies of the TBH were studied using scanning electron microscope of JEOL (JSM 6490 LV). Samples were mounted on aluminum stub with the help of double-sided tape. Mounted stabs were coated with gold palladium prior to analysis using a Polaron sputter coater. The surface area and pore characteristics of adsorbents TBH were determined from nitrogen adsorption/desorption isotherms at 77 K (boiling point of nitrogen gas at 1 atm pressure) using a surface area analyzer (BELSORP-max, Japan).

Point of zero charge (PZC) for TBH

The PZC characteristic of TBH was determined by solid addition method using 0.1 M KCl and 0.002 M citrimide solutions. KCl and citrimide solution (40 mL) was taken in 100 mL Stoppered conical flask. The initial pH values of the solutions were adjusted between 2 and 12 by adding either 0.1N HCl or 0.1N NaOH. The total volume of the solution in each flask was adjusted exactly to 50 mL by adding the KCl and citrimide solution. The initial pH of the solution was then accurately noted. The TBH (0.5 g) was added to each flask. The suspensions were shaken and allowed to equilibrate for two days with intermittent shaking. The final pH values of the supernatant liquid were noted. The difference between the initial and final pH values ($\Delta pH = pH_i - pH_f$) were

plotted against the initial pH value. The point of intersection of the resulting curve at which change in pH is zero gives the PZC.

Adsorption procedure

The adsorption equilibrium was probed by batch technique in 250 mL conical flasks contacting the TBH (1.0 g/L) with 100 mL of phenol solutions of known concentrations (25-1000 mg/L), shaking at 100 rpm for 2h at room temperature (30°C), followed by filtration (0.45 μ) and subsequent analysis of residual phenol concentration in the filtrate (double beam spectrophotometer Carry-100, Australia) at 269, 280 and 322 nm (λ_{max}) respectively. The effect of adsorbent dose, adsorbate concentration, temperature, pH and effect of urea was investigated. For determining the effect of pH on phenol adsorption, initial pH of phenol solutions were adjusted to the desired value (2-10) using 0.1 N HCl or 0.1 N NaOH. The amount of phenols adsorbed by the adsorbent at equilibrium was calculated as follows:-

$$q_e = \frac{(C_o - C_e)V}{m} \quad \dots(1)$$

where C_o and C_e are initial and equilibrium concentrations (mg l^{-1}) of phenols in the solution, V the volume (l), m the weight (g) of the adsorbent and q_e is the amount of phenols adsorbed by the adsorbent at equilibrium (mg g^{-1}).

Results and Discussion

Elemental characterization

The TBH was found to contain C (77.00%), O (18.31%), K (0.01%), Na (0.02%), Al (0.91%), Si (2.20%), P (0.1%) and Ca (1.07%).

FT-IR spectral analysis

The FT-IR spectrum of blank TBH (Fig not shown) exhibited weak and broad peaks in the region of 4000-400 cm^{-1} , which showed the presence of hydroxyl, carbonyl, carboxyl, lactone, aromatic, and cellulosic structures. The band stretch observed in FT-IR spectrum of the TBH at 3644 cm^{-1} is typically of cellulosic -OH group²⁰. Similarly, the characteristic broad peak of carboxylic -OH at 3300-2600 cm^{-1} and the band stretch at 1591.3, and 1557.4 cm^{-1} showed the presence of carboxylate group²⁰, which shifted to 1581.2, 1462.4 and 1587.8 cm^{-1} after the adsorption of studied phenols,

respectively. The other specific area identified in the blank TBH was at 1231.6 cm^{-1} indicating the presence of lactone, which shifted to 1223.5, 1167.9 and 1228.1 cm^{-1} after the adsorption of phenol, *p*-chlorophenol and *p*-nitrophenol, respectively due to hydrogen bonding. These observations indicate the formation of carbonyl groups on carbonization of the TBH. It has been reported^{21,22} that oxidized carbon contains mainly carboxyl, hydroxyl and carbonyl groups. The possible mechanism for phenols adsorption onto TBH was postulated on the basis of functional groups evident from the FT-IR spectral analysis of blank and phenols-adsorbed TBH. It may be concluded that adsorption of phenols onto TBH was through hydrogen bonding mechanism in which Cl atom in *p*-chlorophenol may play a very important role. The Cl, O and H atoms in *p*-chlorophenol can also form hydrogen bonding with the carbonyl and hydroxyl group of the TBH. The electrophilic property of oxygen in $-\text{NO}_2$ of *p*-nitrophenol leads nitrogen atom to difficultly form hydrogen bonding with hydroxyl in the TBH. Even though $-\text{OH}$ group in *p*-nitrophenol may form hydrogen bonding with the carbonyl group of the TBH, it is difficult to lead *p*-nitrophenol to tightly adsorb around the TBH. Similarly, the hydroxyl in phenols may form hydrogen bonding with the carbonyl and hydroxyl group of the TBH which is responsible for occurrence of adsorption. Thus, the adsorption capacity of *p*-nitrophenol and phenol onto the TBH are all lower than that of *p*-chlorophenol. Similar trends of

adsorption of phenol and its derivatives onto functional chitosan have been reported by Li *et al.*²³.

SEM characterization

The SEM images shown in Fig. 1 clearly demonstrate the porosity and surface texture of new adsorbent material.

BET analysis

The BET (Brunauer-Emmett-Teller) surface area (S_{BET}) was measured by means of standard BET equation applied in the relative pressure range of 0.05–0.10. The micropore surface areas (S_{mic}), external surface area (S_{ext}), as well as the micropore volume (V_{mic}) were calculated by the t-plot method. The total pore volume (V_t) and pore radius (R_p) (shown in Table 1) were deduced from the manufacturer's software.

The BET analysis reveals that the TBH had a surface area $454\text{ m}^2\text{g}^{-1}$, which was primarily contributed by micropores. The average pore diameter of TBH was found to be 2.49 nm, which is an indicative of its micropores character defined by IUPAC (International Union of Pure & Applied Chemistry, 2001).

PZC characterization

The surface potential of the adsorbent may be influenced by the *pH* value²⁴ of the coexisting liquid bulk phase. The *pH* value, at which the surface charge is zero, is called the point of zero charge (PZC). The surface will be positively charged at

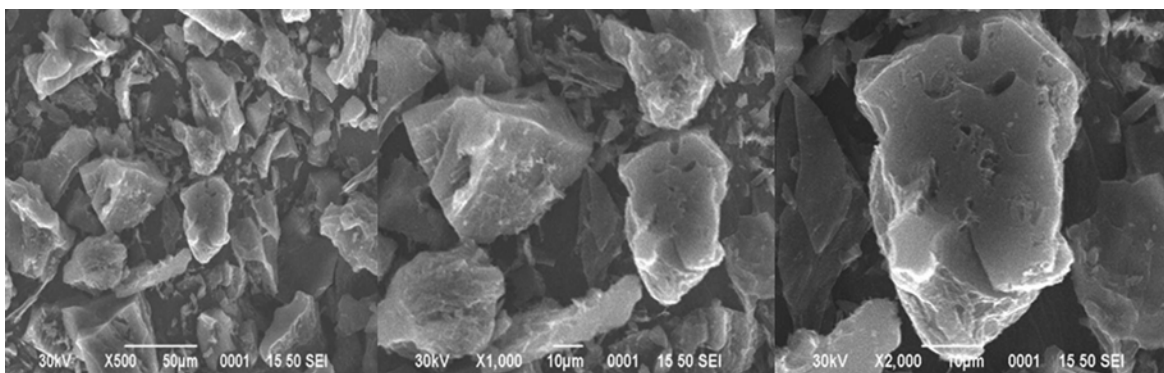


Fig. 1—SEM images of TBH (100 mesh) at different magnifications

Table 1—Surface parameters of TBH

BET method			T-plot method				
(V_{mono}) (cm^3g^{-1})	(S_{BET}) (m^2g^{-1})	(S_{Total}) (m^2g^{-1})	(S_{ext}) (m^2g^{-1})	(S_{mic}) (m^2g^{-1})	(V_{mic}) (cm^3g^{-1})	(V_T) (cm^3g^{-1})	R_p (nm)
104	454	530	4	526	0.220	0.051	2.49

$pH < pH_{PZC}$ and negatively charged at $pH > pH_{PZC}$. Since, pH_{PZC} of the TBH was found to be about 6.8, at any $pH < pH_{PZC}$, the surface of TBH will be positively charged and at $pH > pH_{PZC}$, the surface will be negative.

Adsorption equilibrium

Several equilibrium isotherm equations were applied to optimize of an adsorption system for the adsorption of phenols onto the TBH.

The Freundlich isotherm²⁵ is employed by assuming a heterogeneous surface with a nonuniform distribution of heat of adsorption over the surface may be written as:

$$q_e = K_F C_e^{\frac{1}{n}} \quad \dots(2a)$$

which can be linearized as:

$$\ln q_e = \ln K_F + \frac{1}{n} \ln C_e \quad \dots(2b)$$

where q_e (mg/g) is the amount of solute adsorbed per unit weight of adsorbent, C_e (mg/L) is the equilibrium concentration of solute, K_F (mg/g) is the Freundlich constant which indicates the relative adsorption capacity of the adsorbent and $1/n$ is the constant indicate the intensity of adsorption.

The Langmuir equilibrium isotherm²⁶ is based on the fact that the adsorption occurs at specific homogenous site within the surface of adsorbent and monolayer sorption onto a surface with a finite number of identical sites and there are no interaction between adsorbed molecules on the surface, may be written as:-

$$q_e = \frac{q_m K_L C_e}{1 + K_L C_e} \quad \dots(3a)$$

which can be linearized as:

$$\frac{C_e}{q_e} = \frac{1}{K_L q_m} + \frac{C_e}{q_m} \quad \dots(3b)$$

where q_e (mg/g) is the amount of solute adsorbed per unit weight of adsorbent, C_e (mg/L) is the equilibrium concentration of solute, q_m is the monolayer adsorption capacity (mg/g) and is a constant, and K_L is a constant related to the free energy of sorption ($K_L \propto e^{-\Delta G/RT}$). It is the reciprocal of the concentration at which the adsorbent is half-saturated. Using plot of experimental data as C_e/q_e vs $1/q_m$ (Fig. not shown) values of the constants were evaluated.

The Redlich–Peterson²⁷ (R–P) equation is a three parameter model and can be applied to homogenous and heterogeneous system and given as:

$$q_e = \frac{K_R C_e}{1 + \alpha_r C_e^\beta} \quad \dots(4a)$$

which can be linearized as:-

$$\ln \left(K_R \frac{C_e}{q_e} - 1 \right) = \ln a_r + \beta \ln C_e \quad \dots(4b)$$

where K_R ($\text{dm}^3 \text{g}^{-1}$) and a_r ($\text{dm}^3 \text{mg}^{-1}$) is R–P isotherm constant and β is the exponent having values between 0 and 1. Since K_R is unknown in linear R–P equation which can be fitted to experimental data by maximizing R^2 (regression coefficient) between predicted value of q_e from Eq. 4(b) and the experimental data using the solver add-in function of datafit-9 program.

The Temkin isotherm²⁸ is given as:

$$q_e = \frac{RT}{b} \ln(K_T C_e) \quad \dots(5a)$$

which can be linearized as:

$$q_e = B_1 \ln K_T + B_1 \ln C_e \quad \dots(5b)$$

where $B_1 = RT/b$, b is the Temkin energy constant (J mol^{-1}). The factor K_T in this isotherm explicitly takes into account the interactions between adsorbing species and the adsorbent. A plot of q_e vs $\ln C_e$ enables the determination of the isotherm constants b , B_1 and K_T from the slope and intercept, respectively. All constants were calculated with the help of DataFit-9 software.

The standard deviation and standard error in each case was determined using the equation:

$$\text{Standard Deviation} = \sqrt{\frac{\sum(X - \bar{X})^2}{n-1}} \quad \dots(6)$$

and

$$\text{Standard error} = \frac{s}{n} \quad \dots(7)$$

where s is standard deviation, n is the total number of samples, \bar{X} is the average of the sample, X is the value of each sample.

The comparative nonlinear plots for phenols using different isotherm models given in Fig. 2. clearly showed that the Langmuir isotherm model was found best fitted among studied models.

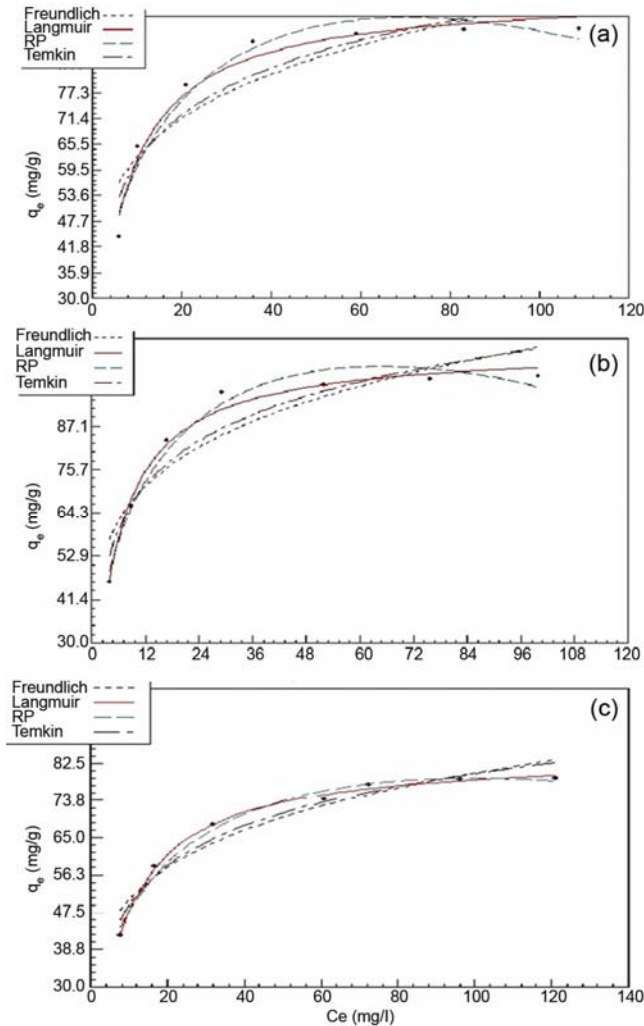


Fig. 2—Plots illustrating different isotherms for (a) phenol, (b) *p*-chlorophenol and (c) *p*-nitrophenol adsorption onto the TBH at 30°C

The linear and non linear regression coefficient showed that the Langmuir model was better fitted model in the sorption behavior of phenols from the aqueous solution onto the TBH than other adsorption isotherm models. It was assumed that the monolayer sorption takes place onto an adsorbent surface with a finite number of identical homogeneous sites defined by Langmuir equation. Different isotherm parameters were tabulated in Table 2.

Kinetics of adsorption

Adsorption kinetics was studied by monitoring the progress of the adsorption process at different time intervals. Figure 3 clearly demonstrates that the amount of adsorption was found to increase up to nearly 90 min and finally attained a constant value upto 200 min. Several kinetic models were tested with

observed experimental results in order to describe the mechanism of adsorption process. The results of the two models are represented on the Figs. 4 and 5. The kinetic parameters of each model are tabulated in Table 3.

The Lagergeren first order rate expression²⁹ is written as:-

$$\log(q_e - q_t) = \log q_e - \frac{k_{ad}}{2.303} t \quad \dots(8)$$

where q_t and q_{eq} are the amount adsorbed at time t and at equilibrium, t is time K_{ad} is rate constant for adsorption.

A $\log(q_e - q_t)$ vs. time plots give a straight line, (Fig. 4.) K_{ad} was calculated from the slope at different temperature and data are presented in Table 3.

The pseudo second order kinetic equation²⁹ is given as:

$$\frac{dq_t}{dt} = K_2 (q_e - q_t)^2 \quad \dots(9a)$$

The integration of the equation leads to:

$$\frac{t}{q_t} = \frac{1}{K_2 q_e^2} + \frac{1}{q_e} t \quad \dots(9b)$$

where K_2 is the rate constant ($\text{g mg}^{-1} \text{min}^{-1}$)

The slope and intercept of the plot between t/q_t vs $1/t$ gives the value of q_e and K_2 , respectively and are shown in Table 3.

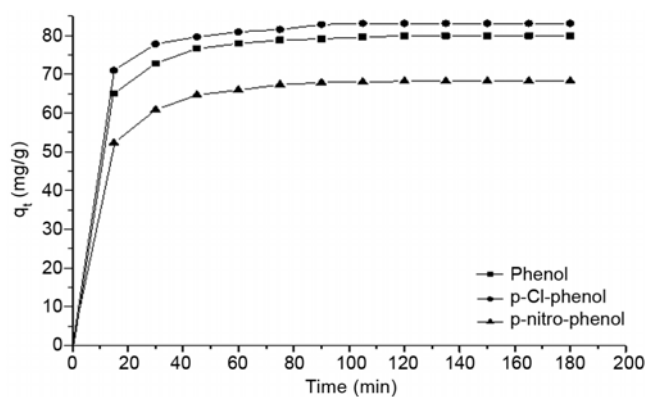
The data shown in Table 3 illustrated that the first-order kinetic equation does not represent the experimental adsorption data satisfactorily. However, the second-order kinetic model represents the adsorption data well with $R^2 = 0.99$ obtained from both the linear and nonlinear regression methods. Such representative plots are shown in Figs. 4 and 5, respectively.

Effect of surface functionalities and pH of solution

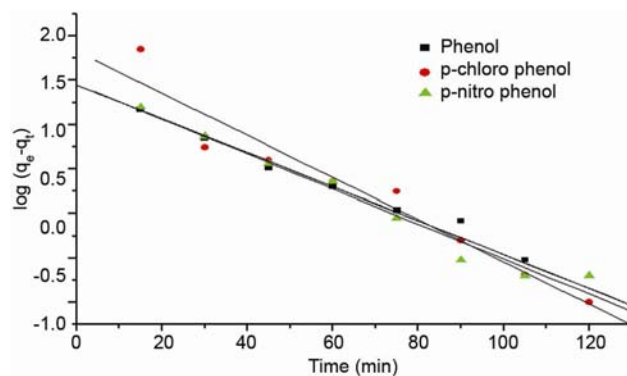
It has been reported¹⁴ that in solution, phenols behave as weak acid (pK_a of phenol, *p*-chlorophenol and *p*-nitrophenol are 9.89, 9.37 and 7.15, respectively). The initial pH of adsorption medium is one of the most important parameters affecting the adsorption process. At $pH \geq 10$, the phenols dissociate and phenolate anions are formed, while the surface functional groups are either neutral or negatively charged^{30,31}. The electrostatic repulsion between the identical charges lowers the adsorption capacities in the case of phenol, *p*-chlorophenol and

Table 2—Parameters of adsorption isotherms of phenols onto the TBH

	Phenol	<i>p</i> -Chloro phenol	<i>p</i> -Nitro phenol
Langmuir Isotherms			
K_L	0.20	0.23	0.13
q_m	97.52	105.24	84.43
R^2 (linear)	0.99	0.99	0.99
R^2 (Non linear)	0.98	0.98	0.99
Standard error	3.50	2.609	0.845
Freundlich Isotherm			
K_f	40.07	43.85	31.70
$1/n$	0.19	0.195	0.20
R^2 (linear)	0.82	0.84	0.92
R^2 (non linear)	0.82	0.85	0.92
Standard Error	8.47	8.82	4.174
Temkin Isotherm			
B	15.72	16.88	13.50
K_T	4.95	5.75	3.78
R^2 (linear)	0.87	0.91	0.96
R^2 (non linear)	0.87	0.91	0.957
Standard Error	7.08	6.96	3.10
Redlich-Peterson Model			
K_R	24.95	29.43	21.42
a_R	-1.14	-1.24	-0.51
β	0.46	0.44	0.39
R^2 (linear)	0.95	0.97	0.98
R^2 (non linear)	0.96	0.98	0.98
Standard Error	34.6	3.80	1.97

Fig. 3—A plot of q_t vs. time (min)

p-nitrophenol. The effect of *pH* can also be explained using pH_{ZPC} of the adsorbent. In the present study, the pH_{ZPC} of TBH is 6.8. At any *pH* below pH_{ZPC} , the surface of the adsorbent is positively charged and at *pH* above pH_{ZPC} , the surface is negatively charged. The adsorption of phenols on TBH shows that adsorption decreases with increasing *pH*. The *pH* primarily affects the degree of ionization of phenols and the surface properties of the TBH. At low *pH*

Fig. 4—Lagergren plots for the adsorption of phenol, *p*-chlorophenol and *p*-nitrophenol onto TBH (*pH* 7.0, TBH 1 g/L and 30°C)

values, the surface of TBH would be protonated and resulted in a stronger attraction for aromatic ring and electronegative group of phenols. At high *pH*, OH^- ions would compete with the phenolate ion for sorption sites³². Sorption of excess of OH^- ions could convert an initial positively charged surface of TBH into a negatively charged surface resulting repulsion of negatively charged phenolates ions and thus

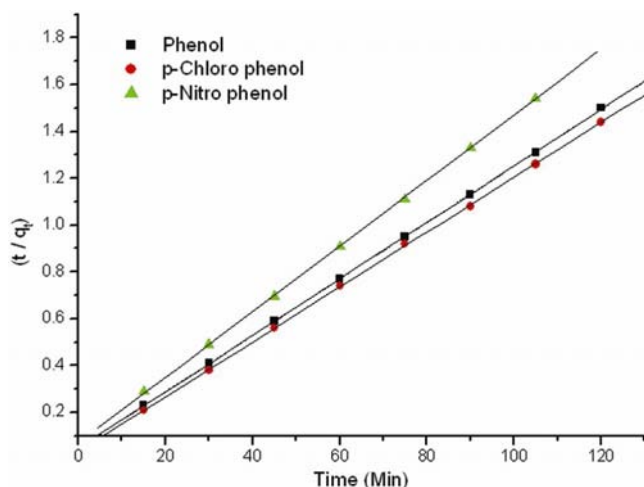


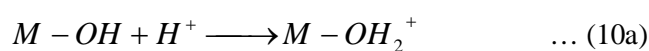
Fig. 5—Pseudo second order plots for the adsorption of phenol, *p*-chlorophenol and *p*-nitrophenol onto TBH (*pH* 6.0, TBH 1 g/L and 30°C)

Table 3—Kinetics parameters for adsorption of phenols onto the TBH

	Lagrangien's model		
	K_f (min^{-1})	q_e (mg/g)	R^2
Phenol	0.083	4.26	0.98
Chlorophenol	0.054	6.22	0.94
Nitrophenol	0.0453	4.29	0.97
	Kinetic model of the pseudo second order		
	K_2 ($\text{g mg}^{-1} \text{min}^{-1}$)	q_e (mg/g)	R^2
Phenol	0.055	82.94	0.999
Chlorophenol	0.063	85.42	
Nitrophenol	0.0027	71.42	0.999

adsorption decreased. This could also be due to the increased solubility of phenol in alkaline conditions, which results in greater affinity for the phenol molecules to remain in solution rather than to get adsorbed onto the carbon surface. Unionized phenol molecules would also be attracted, possibly, by physical force (H-bonding).

When the solution *pH* is lowered than pH_{ZPC} , the undissociated phenols molecules are more easily attracted by the positively charged surface of adsorbent, favoring the accumulation of phenols molecules on the surface and thus promoting adsorption. On the other hand, when the solution *pH* exceeded pH_{ZPC} , the phenolate ions are repelled by the negative charged surface of adsorbent, hence, adsorption is decreased³³⁻³⁵.



It was observed that TBH has a maximum affinity toward phenols at *pH* ~ 6.0 to 8.0. It appears that the dominant sorption process takes place in molecular forms of phenols at lower *pH* is perhaps given by Eq. 10(a). Other reactions given by Eq. 10(b) plays an insignificant role in the overall adsorption of phenol onto the TBH. It may be noted that the solution *pH* varies with contact time with the addition of TBH. It is found that the solution *pH* (*pH* = 6.0) increases instantaneously to about 8.0 after the addition of the optimum amount of TBH, rises to about 8.0 (i.e. nearer pH_{ZPC} ~ 6.8) after 6 h and remains constant thereafter.

Thermodynamics of titled adsorbate-adsorbent system

The effect of temperature on the adsorption behavior of the TBH has been studied in the range of 10-60°C. At very low temperature *i.e.* 10°C, the adsorption phenomenon was very slow, at moderate temperature (30-40°C) adsorptions gradually increases and then decreases. It is anticipated that temperature is required for the breaking of hydrogen bonding between phenols and water molecules which first enhanced the rate of adsorption at moderate temperature. Data (Table 4) demonstrates an endothermic nature of the process. Thermodynamic parameters were calculated as follows:

Gibbs free energy change ΔG^0 was calculated³⁶ using the equation $\Delta G^0 = -RT \ln K_L$ where K_L is the Langmuir constant at temperature 30°C. Since, the Langmuir isotherm has been found to well represented ($R^2 = 0.99$) the equilibrium sorption data. The Langmuir constant K_L has been used to determine the thermodynamic parameters from given equations.

The Gibbs free energy³⁷ change is also related to enthalpy and entropy as:

$$\Delta G^0 = \Delta H^0 - T\Delta S^0 \quad \dots(11)$$

Apparent heat of adsorption enthalpy, ΔH^0 and ΔS^0 was evaluated using the equation:

$$\ln K_L = \frac{-\Delta G^0}{RT} = \frac{\Delta S^0}{R} - \frac{\Delta H^0}{RT} \quad \dots(12)$$

The slope and intercept of the plot between $\ln K_L$ vs $1/T$ gives the value of ΔH^0 and ΔS^0 , respectively.

The van't Hoff plot for the Langmuir isotherms is shown in Fig. 6. The thermodynamic data are presented in Table 4.

Table 4—Thermodynamic parameters for adsorption of phenols onto the TBH at 30°C

	ΔH^0 (kJ/mol)	ΔS^0 (kJ/molK)	$-\Delta G^0$ (kJ/mol)					
			283°K	293°K	303°K	313°K	323°K	333°K
Phenol	13.02	0.082	9.91	11.22	13.34	13.51	12.62	13.47
Chlorophenol	11.64	0.080	10.70	11.85	13.7	13.91	13.46	14.05
Nitrophenol	6.04	0.060	10.83	12.35	12.26	12.85	13.05	14.01

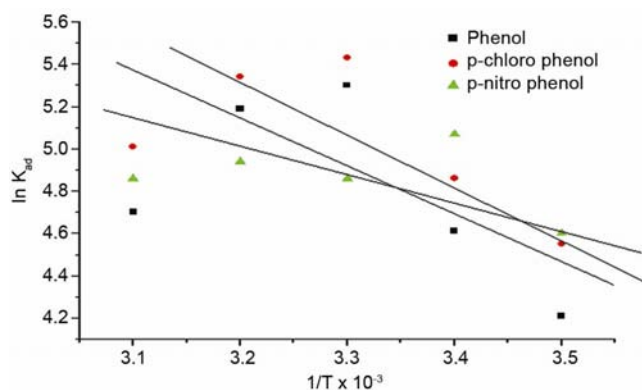


Fig. 6—van't Hoff plots for studied phenols

The endothermic nature of the adsorption was confirmed by the thermodynamic parameters as shown in Table 4. The negative value of ΔG^0 is an indication of the spontaneous nature of the process. Apparent enthalpy of adsorption, ΔH^0 also confirms the endothermic nature of the adsorption process.

Effect of ionic strength

In the present study, the influence of the ionic strength on the amount of the adsorption was investigated. It is anticipated that the hydrophobic force could be the primary driving force for the adsorption of phenol onto TBH. If a hydrophobic interaction makes a significant contribution to adsorption of phenol onto TBH, the adsorption density would have increased with the addition of salt due to "salting out effect"^{37,38}. It was found that the adsorption capacity of phenols exhibits an appreciable increase with addition of KCl. A possible cause is the adsorption of H₂O onto adsorbent. Due to the presence of hydroxyl groups in adsorbent, water cluster might be formed on the surface by hydrogen bonding, which can interface the adsorption of phenols. In the presence of KCl, water cluster can be demolished. Hence, the adsorption capacity of phenols increases.

Effect of urea

To explore the role of hydrogen bonding, adsorption tests were executed in the presence of urea, a hydrogen bond breaker. Adsorption was reduced in

the presence of urea suggesting the role of hydrogen bonding in the present case.

Conclusion

The TBH; produced from water caltrop demonstrates high potential for effective removal of phenol and its derivatives from waste water. The various equilibrium models such as Freundlich, Langmuir, Redlich-Peterson and Temkin are tested to describe the equilibrium adsorption. However, Langmuir isotherm is found most suitable as representative of the equilibrium adsorption data. The kinetic modeling of the phenols adsorption onto TBH indicates that adsorption process is pseudo-second order with the correlation coefficients higher than 0.99. Thermodynamic calculations indicate that the sorption process is spontaneous and endothermic. The adsorption properties of studied adsorption system depend on several factors such as pK_a , polarity and solution condition such as pH, ionic strength and adsorbate concentration. The precursor employed for the preparation of the activated carbon (TBH) is widely available and inexpensive. Hence, scalable for industrial purpose.

Acknowledgements

The authors express their thanks for the support of USIC, Babasaheb Bhimrao Ambedkar University (A Central University), India for FT-IR and SEM analysis. The Financial support to BC from UGC-JRF (17-1/2006 SA-1) is gratefully acknowledged.

References

- 1 Sobiesiak M & Podkoscielna B, *Appl Surf Sci*, 257 (2010) 1222.
- 2 Beker U, Ganbold B, Dertli H & Gulbayir D D, *Energy Convers Manage*, 51 (2010) 235.
- 3 Agency for Toxic Substances and Disease Registry (ATSDR), *Toxicological profile for phenol*, Atlanta, GA: U.S. Department of Health and Human Services, Public Health Service (1998).
- 4 Kumakiri I, Hokstad J, Peters T A, Melbye A G & Rader H, *J Petrol Sci Eng*, 79 (2011) 37.
- 5 Fan J, Fan Y, Pei Y, Wu K, Wang J & Fan M, *Sep Purif Technol*, 61 2008 324.

- 6 Yan J, Nanqi R, Xun C, Di W, Liyan W & Sen L, *Chin J Chem Eng* 16 (2008), 796.
- 7 Aravindhhan R, Rao J R & Nair B U, *J Environ Manage* 90 (2009) 1877.
- 8 Bayramoglu G, Gursel I, Tunali Y & Arica M Y, *Bioresource Technol*, 100 (2009) 2685.
- 9 Ioannou Z & Simitzis J, *J Hazard Mater*, 171 (2009) 954.
- 10 Muhammad A, *Adv Colloid Interf Sci*, 143 (2009) 48.
- 11 El-Sheikh A H, Newman A P, Said A J, Alzawahreh A M, Abu-Helal M M, *J Environ Manage*, 118 (2013) 1.
- 12 Nayak P S & Singh B K, *Desalination*, 207 (2007) 71.
- 13 Lin S H & Juang R S, *J Environ Manage*, 90 (2009) 1336.
- 14 Dabrowski A, Podkoscielny P, Hubicki Z & Barczak M, *Chemosphere*, 58 (2005) 1049.
- 15 Dasa L, Kolar P, Classena J J & Osborne J A, *Indust Crops Prod*, 45 (2013) 215.
- 16 Kilic M, Varol E A & Putun A E, *J Hazard Mater*, 189 (2011) 397.
- 17 Kalderis D, Koutoulakis D, Paraskeva P, Diamadopoulos E, Otal E & Olivares del Valle J, *Chem Eng J*, 144 (2008) 42.
- 18 Mohan D, Singh K P & Singh V K, *J Hazard Mater*, 152 (2008) 1045.
- 19 Achak M, Hafidi A, Ouazzani N, Sayadi S & Mandi L, *J Hazard Mater*, 166 (2009) 117.
- 20 Mubarik S, Saeed A, Mehmooda Z & Muhammad I, *J Taiwan Ins of Chem Eng*, 43 (2012) 926.
- 21 Coughlin R W & Ezra F S, *Environ Sci Technol*, 2 (1968) 291.
- 22 Rathinam A, Rao J R & Nair B U, *J Taiwan Inst Chem Eng*, 42 (2011) 952.
- 23 Li J-M, Meng X-J, Hu C-W & Du J, *Bioresource Technol*, 100 (2009) 1168.
- 24 Singh K, Bharose R, Verma S K & Singh V K, *J Sci Food Agri*, 93 (2012) 1.
- 25 Freundlich H, *Z Phys Chem*, 57 (1907) 385.
- 26 Langmuir I, *J Am Chem Soc*, 40 (1918) 1361.
- 27 Redlich O & Peterson D L, *J Phys Chem*, 63 (1959) 1024.
- 28 Mohan D, Singh K P, Sinha S & Ghosh D, *Carbon*, 43 (2005) 1680.
- 29 Lataye D H, Mishra I M, Mall I D, *Indus Eng Chem Res*, 45 (2006) 3934.
- 30 Nadavala S K, Swayampakula K, Boddu V M & Abburi K, *J Hazard Mater*, 162 (2009) 482.
- 31 Kumar N S & Min K, *Chem Eng J*, 168 (2011) 562.
- 32 Hameed B H, Rahman A A, *J Hazard Mater*, 160 (2008) 576.
- 33 Dursun A Y & Kalayci C S, *J Hazard Mater*, 125 (2005) 151.
- 34 Beker U, Ganbold B, Dertli H & Gu' Ibayir D D, *Energ Convers Manage*, 51 (2010) 235.
- 35 Altendor S, Carene B, Emmanuel E, Lambert J, Ehrhardt J-J & Gaspard S, *J Hazard Mater*, 165 (2009) 1029.
- 36 Singh K & Mohan S, *J Colloid Interf Sci*, 270 (2004) 21.
- 37 Singh K & Mohan S, *Appl Surf Sci*, 221 (2004) 308.
- 38 Arafat H A, Franz M & Pinto N G, *Langmuir*, 15 (1999) 5997.